

Relationship between defect energies and embedded-atom-method parameters

R. A. Johnson

Department of Materials Science, Thornton Hall, University of Virginia, Charlottesville, Virginia 22901

(Received 19 October 1987)

The parameter dependence of vacancy and self-interstitial formation energies has been studied with an analytic nearest-neighbor atomistic model based on the embedded-atom method. The model was designed for fcc copper, but the results should not depend on either the structure or the element. Exponentially decreasing functions were used for both the electron density function and the two-body interaction. Energies were dependent on the cutoff procedure for these functions between first and second neighbors, but the conclusions indicate trends and are quite general. Defect energies (vacancy and self-interstitial) were found to have negligible dependence on the cohesive energy, vary only slightly with the bulk modulus, but to be linearly proportional to the average shear modulus. Defect energies were insensitive to variations in the exponent parameters if their average was held constant and thus to whether the two-body potential was attractive or repulsive. Vacancy energies decreased while interstitial energies increased with an increase in the average of the exponent parameters.

INTRODUCTION

An analytic nearest-neighbor model for fcc metals based on the embedded-atom method (EAM)^{1,2} has recently been developed.³ This model was applied to defects for which there is little change in energy with relaxation, so that the unrelaxed energy provides a good approximation to the fully relaxed case. The dependence of the defect energies on various physical input parameters was then studied.

A set of calculations for vacancies, self-interstitials, and small clusters, in which relaxation is significant, has been carried out with this model. As in the earlier report, the emphasis is on the implications of the mathematical format of EAM.

Details of the model and references are given in Ref. 3 and will not be repeated in detail here. In EAM, an atomic electron density function $f(r)$, a two-body potential $\phi(r)$, and an embedding function $F(\rho)$ must be provided. In the present model, both $f(r)$ and $\phi(r)$ are taken as exponentially decaying functions, and $F(\rho)$ is determined from a universal energy curve of energy versus lattice constant given by Rose *et al.*⁴ Model parameters are obtained by fitting to physical properties such as the lattice constant, the cohesive energy, the vacancy formation energy, and elastic properties.

The mathematical formulation of the present model is then

$$f(r) = f_e \exp \left[-\beta \left(\frac{r}{r_e} - 1 \right) \right], \quad (1)$$

$$\phi(r) = \phi_e \exp \left[-\gamma \left(\frac{r}{r_e} - 1 \right) \right] \quad (2)$$

$$F(\rho) = -E_c \left[1 - \frac{\alpha}{\beta} \ln \left(\frac{\rho}{\rho_e} \right) \right] \left[\frac{\rho}{\rho_e} \right]^{\alpha/\beta} - \Phi_e \left[\frac{\rho}{\rho_e} \right]^{\gamma/\beta}, \quad (3)$$

where r_e is the nearest-neighbor equilibrium distance, E_c is the cohesive energy, and α is $3(\Omega B/E_c)^{1/2}$ with Ω the atomic volume and B the bulk modulus. The electron density experienced by some atom i and the bond energy associated with this atom are given by sums over neighboring atoms:

$$\rho_i = \sum_j' f(r_{ij}), \quad (4)$$

$$\Phi_i = \frac{1}{2} \sum_j' \phi(r_{ij}), \quad (5)$$

and the subscript e indicates evaluation at the equilibrium value. For this nearest-neighbor fcc model, $\rho_e = 12f_e$ and $\Phi_e = 6\phi_e$. The crystal energy is then just the sum of the energies of the individual atoms, i.e.,

$$E = \sum_i (F_i + \Phi_i). \quad (6)$$

The parameter f_e cancels from the model, and ϕ_e is related to the average shear modulus G by

$$\phi_e = 5\Omega G / [2\gamma(\gamma - \beta)]. \quad (7)$$

For a specific metal, values of E_c , B , G , r_e , β , and γ are required, as well as information about the cutoff between first- and second-neighbor distances. β is obtained by fitting to the atomic electron density and γ by approximate fitting to the unrelaxed vacancy formation energy.

CALCULATIONS

In Ref. 3, the electron density function $f(r)$ and the two-body potential $\phi(r)$ were cut off in an unspecified manner between first- and second-neighbor distances in the fcc lattice and the results were insensitive to this choice. Calculations with significant changes in the atomic configurations are affected by the cutoff procedure, however, and three methods were used in the present work. First (case a), the functions $f(r)$ and $\phi(r)$

were simply truncated at a cutoff distance r_c . Both energies and forces are discontinuous with this scheme. Secondly (case b), these functions were decreased by a constant so that their value at r_c was zero. This eliminates the discontinuities in energies, but leaves the forces discontinuous. In case c, quadratic factors were added to these functions and were adjusted for zero value and slope at r_c and for matching value and slope to the exponential functions at match point distances r_β and r_γ determined by the fitting for $f(r)$ and $\phi(r)$, respectively. Both of these distances are greater than the nearest-neighbor distance in the present case, so that the electron density function and two-body potential are unchanged at nearest-neighbor distances, and smoothly go to zero value with zero slope at distances less than second neighbor. The two-body potential is shown in Fig. 1 for the three methods using the parameter values for copper in Ref. 3 and $r_c = 3.45 \text{ \AA}$ (about 84% of the distance between first and second neighbors).

The embedding function in the present model is based on fitting to the universal equation of state given by Rose *et al.*⁴ and it is altered by any change in the electron density or two-body potential functions. This variation is seen in Fig. 2 for the three cases with the same copper parameter values as used in Fig. 1. In case a, the embedding function is not defined for $\rho < \rho_e \exp\{-\beta[(r_c/r_e) - 1]\}$, which corresponds to the density at an atom site in the perfect crystal if the nearest-neighbor distance is expanded to r_c . This part of the curve is never used in these defect calculations. The finite value of $F(\rho)$ at $\rho = 0$ in cases b and c occurs because the universal energy curve is not zero at the cutoff distance at which ρ is zero.

All three cases fit the perfect-crystal parameters exactly: E_c and ΩB are inputs for determining the embedding function, equilibrium is maintained at the input r_e , and β and γ are held fixed. Since shear is only dependent on the slopes and curvatures of $f(r)$ and $\phi(r)$ at the equilibrium distance, G is also unaltered in going from case a to cases b and c. However, the unrelaxed vacancy forma-

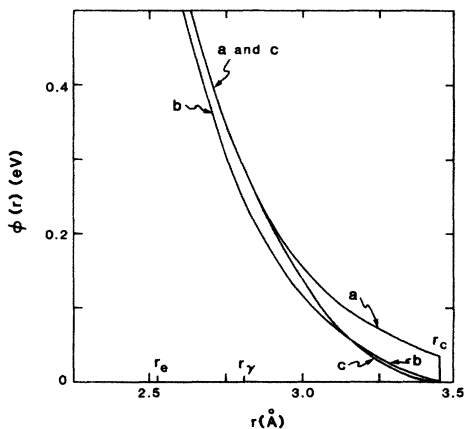


FIG. 1. The two-body potentials for the three cutoff mechanisms. Case a is truncation at cutoff distance r_c , case b involves subtracting a constant from case a, and case c requires fitting a parabola to case a at r_γ . The nearest-neighbor distance is r_e .

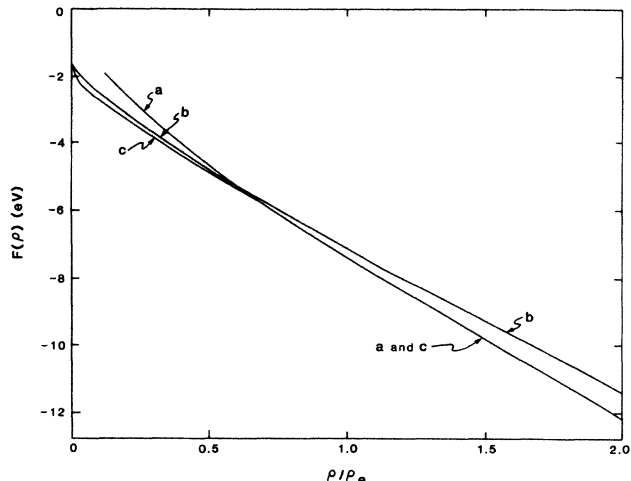


FIG. 2. The embedding functions for the three cutoff mechanisms. The embedding function outside the range $0.5 < \rho/\rho_e < 1.5$ is not used in the present defect calculations.

tion energy, which is an input in case a used to determine γ and is maintained in case c, is not matched in case b. Numerous runs were made in which the physical parameters E_c , B , G , r_e , β , and γ were varied, and the effects of varying r_c and the cutoff form have been studied.

The relaxation calculations were carried out with the computer code DYN52 developed at Sandia National Laboratory, Livermore,⁵ Cubic sets of 108 atoms and 256 atoms were used for vacancy and interstitial calculations, respectively. Energy minimization was obtained with the conjugate gradient method,⁶ and periodic boundary conditions were applied. Volume change is determined with this method and permits the use of such small sets of atoms. In a typical case, the change in interstitial energy was insignificant when the smaller 108-atom set was used. However, if volume change is not allowed, the interstitial energy increased by 0.06 eV with the 256-atom set and 0.15 eV with the 108-atom set.

RESULTS

Cutoff mechanism

The energies of a number of point defects for the three basic cases with $r_c = 3.45 \text{ \AA}$ are given in Table I. The stable and saddle-point configurations for migration for single vacancies and divacancies are V_1 , V_1^* , V_2 , and V_2^* , respectively. The single-vacancy formation energy is fixed at the experimental value of 1.30 eV (Ref. 7) in case a, which carries over to case c. The self-diffusion energy is 2.07 eV,⁸ which corresponds to the formation energy of the vacancy saddle point, while the energies of the other listed defects are not well known experimentally. It is commonly accepted that the divacancy migration energy is less than the single-vacancy migration energy in fcc metals. Since self-diffusion occurs by a vacancy mechanism, the formation energies of the interstitial configurations should be significantly higher than the vacancy energies.

TABLE I. Defect formation energies, in eV, for the three cutoff mechanisms with $r_c = 3.45 \text{ \AA}$.

Defect		Case a	Case b	Case c
Vacancy, stable	V_1	1.30	0.90	1.30
Vacancy, saddle point	V_1^*	1.75	1.70	2.45
Divacancy, stable	V_2	2.41	1.67	2.41
Divacancy, saddle point	V_2^*	2.87	2.34	3.31
Interstitial, [100] split	H_O	2.09	2.68	3.26
Interstitial, octahedral	O	1.91	2.82	4.00
Interstitial, possible H_O^* :	OC	2.09	2.79	3.56

The notation for self-interstitials is that used by Johnson⁹ with H_O the split octahedral or [100] split, O the octahedral, and OC a local minimum on the line connecting an octahedral and a crowdion site. If H_O is the lowest-energy interstitial configuration as is commonly found, then OC is a likely saddle-point configuration for migration.

Case a, in which energy and force are both discontinuous at the cutoff distance, does not fit the experimental pattern well: the vacancy migration energy is too small, the divacancy migration energy is very similar to the single-vacancy value, and the interstitial energies are too small. As will be discussed later, more realistic values are obtained with variations in the physical parameters. The pattern for case b, in which only the force is discontinuous, is better in that the vacancy and divacancy migration energies are reasonable while the vacancy and divacancy formation energies and interstitial formation energies are somewhat small. Again, variations in the physical parameters can yield improved results. In case c the vacancy and divacancy migration energies show the correct relation but are too large, and the interstitial energies are larger than expected. The embedding function is unchanged near the equilibrium electron density in going from case a to case c and only this part is used in the defect calculations. Both the two-body potential and the

electron density are lowered with this shift, but the configuration energies increase. The decrease in the two-body energy is more than compensated by the increase in the embedding energy due to lower electron density.

Cutoff distance

The results for case a are very sensitive to an increase in the cutoff distance, with an increase in r_c from 3.45 to 3.50 \AA decreasing formation energies of six interstitials (the first six listed in Table II) by an average of 16%, for example. Decreasing r_c to 3.35 \AA , twice as large a change, only increases this same set of energies by an average of 2.6%, i.e., there is a relative plateau in defect configuration energies as a function of cutoff distance with $r_c = 3.45 \text{ \AA}$ a satisfactory choice.

The decrease in case b for the same six interstitial configurations with twice as large an increase in r_c averaged 13%, while a decrease in r_c from 3.45 to 3.35 \AA gave an average increase in interstitial energies of 6.6%. Thus the same general pattern is found as in case a, but the plateau is altered to a more continuous slope.

The full set of configurations was not investigated with case c, but enough runs were made to determine that the pattern is similar to that of case b. However, the variation with cutoff is somewhat greater than with case b,

TABLE II. Defect formation energies, in eV, for two cutoff mechanisms with parameters modified as discussed in the text. Results of Foiles *et al.* are shown for comparison. Defect notation from Johnson [R. A. Johnson, Phys. Rev. **145**, 423 (1966)] is used, and the two di-interstitials involve H_O single interstitials at nearest-neighbor sites with the axes of the configurations parallel and perpendicular, respectively, as shown in Figs. 2(a) and 2(b) of Johnson [R. A. Johnson, Phys. Rev. **152**, 629 (1966)].

Defect		Case a	Case b	Foiles <i>et al.</i> ^a
Vacancy, stable	V_1	1.28	1.10	1.28
Vacancy, saddle point	V_1^*	2.02	2.07	2.00
Divacancy, stable	V_2	2.36	2.03	2.29
Divacancy, saddle point	V_2^*	2.99	2.82	2.67
Interstitial, [100] split	H_O	3.16	3.26	2.76
Interstitial, octahedral	O	3.31	3.43	
Interstitial, [111] split	H_T	3.52	3.46	
Interstitial, tetrahedral	T	3.77	3.71	
Interstitial, [110] split	H_C	3.39	3.55	
Interstitial, crowdion	C	3.50	3.57	
Interstitial, possible H_O^*	OC	3.42	3.40	2.85
Di-interstitial, parallel	I_{2A}	5.09	5.54	
Di-interstitial, perpendicular	I_{2B}	5.73	5.64	

^aS. M. Foiles, M. I. Baskes, and M. S. Daw, Phys. Rev. B **33**, 7983 (1986).

even though case c is continuous in both energy and force.

From the results given above, as well as from other runs with different sets of the physical parameters E_c , B , G , r_e , β , and γ in which the cutoff distance was also varied, $r_c = 3.45 \text{ \AA}$ has been adopted as the best compromise. The cutoff is too close to the second-neighbor distance with larger values (the model has been designed to match the perfect crystal with nearest-neighbor interactions only) and the magnitude of the cutoff is too great with smaller values.

The conclusion here is that there is considerable arbitrariness in this short-range model because the results vary with the cutoff mechanism and cutoff distance. They are incorporated into the model to obtain a simple scheme in which the effects of varying the physical parameters can be studied. Fortunately the results from varying the physical parameters are not dependent on the cutoff procedure.

The Sandia group has used a cutoff procedure similar to the present case b, but the cutoff distance was taken between the third- and fourth-neighbor distances.¹⁰ The functions are much smaller at this distance and thus the effect of the discontinuity in force should be minor compared to the present model for most properties. However, the stacking-fault energy and the relative fcc-hcp stability can depend sensitively on the choice of cutoff distance,¹¹ even at large values.

Parameter variation

It was reported in Ref. 3 that the cohesive energy had a negligible effect on vacancy formation and binding energies and on surface energies. Relaxation calculations for three vacancy and three interstitial configurations (V_1 , V_1^* , V_2 , H_O , O , and OC) were carried out with the same result: varying the cohesive energy by a factor of 1.5 did not change any of these six defect energies by as much as 0.01 eV.

Again, as reported in Ref. 3, the bulk modulus is found to have a minor effect on defect formation energies. Each of the six defect energies was increased by 3–4%, with a 50% increase in B . However, the six defect energies vary approximately linearly with the shear modulus G : increasing G by 48% increased all the energies by 42–44%. Flynn¹² investigated atomic jump rates with a quantum-statistical treatment based on dynamical fluctuations. His result for the vacancy migration energy in cubic crystals can be recast in the form

$$E_V^M \simeq 15\Omega G \epsilon(1-\nu)/(7-10\nu) \quad (8)$$

with ϵ a parameter dependent on crystal structure and ν Poisson's ratio. Since Poisson's ratio varies little from metal to metal, this result indicates the same functional dependence on the shear modulus for vacancy migration as found with the present approach.

The variation of defect energies with β and γ is quite complex and numerous functional forms for fitting the six defect energies with five combinations of these parameters have been tried using least-squares analyses. The form

$$E^F = K_1/\beta\gamma + K_2(\beta + \gamma) \quad (9)$$

has been found to fit these formation energies reasonably well, with K_1 and K_2 being constants which determine the admixture of the two contributions for a particular defect. The first term is dominant for the formation of a single stable vacancy and arises from the decrease in bonding, i.e., similar to two-body bond breaking. Using an analytic expansion, this term was shown to provide a good approximation to the unrelaxed vacancy formation energy in Ref. 3. The second term accounts for the additional repulsion when some atoms are tightly squeezed together. The vacancy migration energy contains about equal contributions from these two terms. For self-interstitials, the second factor dominates both formation and differences between configurations.

The stable vacancy formation energy is therefore almost independent of variations of β and γ if their geometric average is held constant, while interstitial energies are little affected by such variations if the arithmetic average is unchanged. In broadest terms, defect energies vary little if the average value of β and γ , either geometric or arithmetic, is held fixed. For example, with the values $\beta=6$ and $\gamma=8$ as the base, using $\beta=4$ and $\gamma=10$ or $\beta=4$ and $\gamma=12$ had but a minor effect on the defect energies. The numbers depend on case and cutoff, but for one set of parameters, increasing the average by 21% produced an average 25% decrease in three vacancy formation energies and a 7% increase in three interstitial formation energies. Because interstitial formation energies are significantly higher than vacancy formation energies, the actual magnitudes of the changes were comparable.

While the functional dependence of the first term in Eq. (9) was expected from earlier studies,³ the form of the last term was not anticipated. At first, $(\gamma - \beta)$ or just γ alone were tried. However, the present form can be understood with an expansion of the effective potential given in Ref. 3. It was shown that, by adding a term linear in ρ to the embedding function $F(\rho)$, an effective two-body potential of the form

$$\phi_{\text{eff}} = \phi_e \left[e^{-\gamma(r/r_e - 1)} - \frac{\gamma}{\beta} e^{-\beta r/r_e - 1} \right] \quad (10)$$

could be obtained which provides a two-body approximation to the embedded-atom model. Expanding this equation to third order in terms of the fractional decrease of the interatomic separation, i.e., with $\delta = 1 - r/r_e$, yields

$$\phi_{\text{eff}} = \frac{5}{2}\Omega G \left[-\frac{1}{\beta\gamma} + \frac{1}{2}\delta^2 + \frac{1}{6}\delta^3(\beta + \gamma) \right]. \quad (11)$$

The first-order term is zero because of equilibrium, and the second-order term is independent of β and γ . For short interatomic distances, the interaction energy increases proportional to $(\beta + \gamma)$.

Sign of two-body potential

Jacobsen *et al.*¹³ have recently derived an expression for the total energy of a set of atoms based on effective

medium theory (EMT). With approximations to render their results amenable to defect calculations, the "embedded-atom format," i.e., Eq. (1), is obtained for simple metals. Indeed, an fcc nearest-neighbor exponential electron density form is used. Although the format is the same, there are differences in interpretation between EAM and EMT. The two-body potential arises from atomic-core–electron-gas electrostatic attraction in EMT, whereas the two-body potential is taken as a repulsion in the EAM. Also, except in the perfect-crystal case, the electron density is not a simple superposition of contributions from neighboring atoms in EMT, but such a superposition raised to a power close to, but not equal to, one. This occurs due to a charge conservation self-consistency requirement using an atomic sphere approximation in which the spheres overlap but are not space filling.

The expression for ϕ_e is given by Eq. (7) and depends on ΩG , γ , and $(\gamma - \beta)$. Thus, interchanging β and γ changes the sign of ϕ_e : if $\gamma > \beta$, the potential is repulsive and vice versa. Runs were therefore made with this modification, which also alters the embedding function and the electron density. There was little change in vacancy and interstitial formation and migration energies.

This can be understood on two counts. First, neither $\beta\gamma$ nor $\beta + \gamma$ change when β and γ are interchanged, and these are the relevant parameters determining defect energies, as reported above. Secondly, the effective two-body potential, Eq. (10), can be rewritten in the form

$$\phi_{\text{eff}} = \frac{5}{2} \Omega G \left[\frac{e^{-\gamma(r/r_e - 1)}}{\gamma(\gamma - \beta)} + \frac{e^{-\beta(r/r_e - 1)}}{\beta(\beta - \gamma)} \right] \quad (12)$$

which is unchanged by this switch. Thus, to the extent that the effective two-body potential is a first-order approximation to the EAM, interchanging β and γ will not alter the results to first order.

Defect energies

As discussed above and indicated by the results in Table I, none of the three cutoff procedures yields defect energies in the anticipated ranges. In case a, bond breaking is essentially fixed by matching the unrelaxed vacancy formation energy, but bond squeezing energies are too small. Indeed, increasing both the shear constant and γ by 1.38, which does not alter the vacancy formation energy, yields realistic energies for a broad range of defect energies as shown in Table II. Most formation energies are somewhat low in case b. Increasing the shear constant by a factor of 1.24 increases the self-diffusion energy to the

experimental value of 2.07 eV and generally scales all energies upward, also listed in Table II. The results of Foiles *et al.*² using a full long-range model are given for comparison.

SUMMARY

A nearest-neighbor EAM model has been developed using a universal equation of state given by Rose *et al.*⁴ and with both the atomic electron density function and the two-body potential taken as exponentially decreasing functions with exponential parameters β and γ , respectively. The input parameters in the model are the atomic volume Ω (or the nearest-neighbor distance r_e), the cohesive energy E_c , the bulk modulus B , the average shear modulus G , and the two exponential factors β and γ . Radial Hartree-Fock wave functions are used to determine β and the vacancy formation energy for γ .

To define a nearest-neighbor model, a cutoff mechanism between the first- and second-neighbor distances must be specified for the exponential terms, which requires a cutoff distance parameter r_c . Three schemes were tried: truncation, subtracting a constant term, and fitting a parabola. All were affected by the cutoff parameter, but a value of $r_c = 3.45 \text{ \AA}$ was found as the best compromise. Cutoff effects generally increase with shorter distances while second-neighbor effects become significant at longer distances.

The parameter dependence may be summarized as

- (a) the cohesive energy has a negligible effect on defect energies,
- (b) the bulk modulus has a minor effect on defect energies,
- (c) the variation of defect energies with the shear modulus is approximately linear,
- (d) there is little variation in defect energies with β and γ if their average is held constant,
- (e) the two-body potential can be attractive or repulsive with little effect on calculated defect energies,
- (f) vacancy energies are decreased and interstitial energies increased by increasing the average of β and γ .

ACKNOWLEDGMENTS

It is a pleasure to acknowledge stimulating discussions with M. I. Baskes, M. S. Daw, and S. M. Foiles at Sandia National Laboratory (Livermore, CA) and D. J. Oh at the University of Virginia. Support from the U.S. Department of Energy (Office of Basic Energy Sciences, Division of Materials Science), under Grant No. DE-FG05-86ER45246, is gratefully acknowledged.

¹M. S. Daw and M. I. Baskes, *Phys. Rev. B* **29**, 6443 (1984).

²S. M. Foiles, M. I. Baskes, and M. S. Daw, *Phys. Rev. B* **33**, 7983 (1986).

³R. A. Johnson, *Phys. Rev. B* **37**, 3924 (1988).

⁴J. H. Rose, J. R. Smith, F. Guinea, and J. Ferrante, *Phys. Rev. B* **29**, 2963 (1984).

⁵M. S. Daw, M. I. Baskes, and S. M. Foiles (private communication).

⁶J. E. Sinclair and R. Fletcher, *J. Phys. C* **7**, 864 (1972).

⁷R. W. Balluffi, *J. Nucl. Mater.* **69&70**, 240 (1978).

⁸N. L. Peterson, *J. Nucl. Mater.* **69&70**, 3 (1978).

⁹R. A. Johnson, *Phys. Rev.* **145**, 423 (1966).

¹⁰S. M. Foiles and M. S. Daw, *J. Mater. Res.* **2**, 5 (1987).

¹¹R. A. Johnson, *Cryst. Lattice Defects* **1**, 37 (1969).

¹²C. P. Flynn, *Phys. Rev.* **171**, 682 (1968).

¹³K. W. Jacobsen, J. K. Nørskov, and M. J. Puska, *Phys. Rev. B* **33**, 7423 (1987).